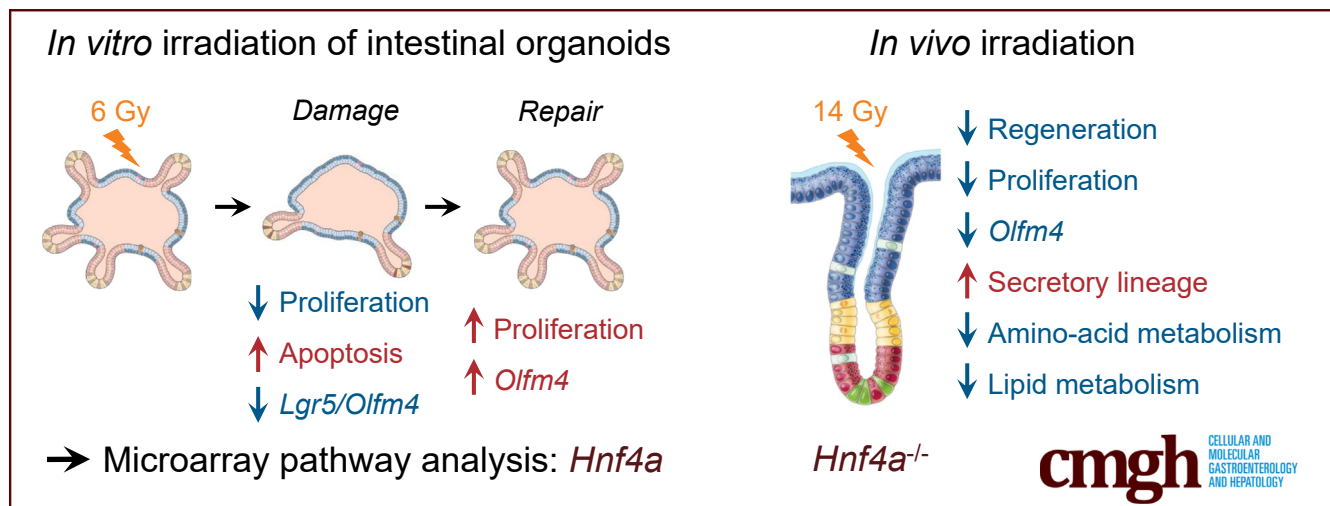


ORIGINAL RESEARCH

A Novel Organoid Model of Damage and Repair Identifies HNF4 α as a Critical Regulator of Intestinal Epithelial Regeneration

Paula S. Montenegro-Miranda,¹ Jonathan H. M. van der Meer,¹ Christine Jones,² Sander Meisner,¹ Jacqueline L. M. Vermeulen,¹ Jan Koster,³ Manon E. Wildenberg,¹ Jarom Heijmans,¹ Francois Boudreau,² Agnes Ribeiro,⁴ Gijs R. van den Brink,^{1,5} and Vanesa Muncan¹

¹Tytgat Institute for Liver and Intestinal Research, Department of Gastroenterology and Hepatology, Amsterdam Gastroenterology and Metabolism, ³Department of Oncogenomics, Cancer Center Amsterdam, Amsterdam UMC, University of Amsterdam, Amsterdam, The Netherlands; ²Département d'Anatomie et de Biologie Cellulaire/Faculté de médecine et des sciences de la santé, Pavillon de Recherche Appliquée sur le Cancer, Sherbrooke, Canada; ⁴Cordeliers Research Center, Sorbonne Université, Université de Paris, INSERM, Paris, France; ⁵Roche Innovation Center Basel, F. Hoffmann-La Roche AG, Basel, Switzerland



SUMMARY

An in vitro damage-repair model by irradiation of primary intestinal epithelial cells was established and validated. This identified hepatocyte nuclear factor 4 α as a regulator of intestinal repair. In vivo knockout of *Hnf4a* confirmed its crucial role in the regeneration process.

BACKGROUND & AIMS: Recent evidence has suggested that the intact intestinal epithelial barrier protects our body from a range of immune-mediated diseases. The epithelial layer has an impressive ability to reconstitute and repair upon damage and this process of repair increasingly is seen as a therapeutic target. In vitro models to study this process in primary intestinal cells are lacking.

METHODS: We established and characterized an in vitro model of intestinal damage and repair by applying γ -radiation on small-intestinal organoids. We then used this model to identify novel regulators of intestinal regeneration.

RESULTS: We identified hepatocyte nuclear factor 4 α (HNF4 α) as a pivotal upstream regulator of the intestinal regenerative response. Organoids lacking *Hnf4a* were not able to propagate in vitro. Importantly, intestinal *Hnf4a* knock-out mice showed impaired regeneration after whole-body irradiation, confirming intestinal organoids as a valuable alternative to in vivo studies.

CONCLUSIONS: In conclusion, we established and validated an in vitro damage-repair model and identified HNF4 α as a crucial regulator of intestinal regeneration. Transcript profiling: GSE141515 and GSE141518. (*Cell Mol Gastroenterol Hepatol* 2020;10:209–223; <https://doi.org/10.1016/j.jcmgh.2020.02.007>)

Keywords: Regeneration; Organoids; Irradiation.

The barrier that separates our body from the intestinal content consists of a single layer of polarized epithelial cells, covered by a thin layer of mucus. To maintain its integrity and ward off colonization by potentially harmful microbes,¹ the homeostatic intestinal epithelium is renewed continuously from a pool of stem cells. When

damaged, the epithelium has a remarkable ability for repair. For example, we and others have found that when almost all stem cells are lost from the intestinal epithelium of a mouse by an induced genetic mutation, it takes only approximately 72 hours for the epithelial layer to entirely repopulate from the few wild-type cells that have escaped genetic recombination.^{2,3} The mechanisms that underlie that remarkable plasticity of the epithelial layer have not been fully defined.

The important role of the epithelial barrier in health and disease has been underscored by recent findings that it has a pathophysiological relevance well beyond intestinal diseases such as inflammatory bowel disease. It has become increasingly clear that a defective epithelial barrier can predispose to a wide range of extraintestinal diseases such as steatohepatitis,⁴ IgA nephropathy,⁵ and systemic lupus erythematosus.⁶ The mechanisms that maintain epithelial barrier function and facilitate its repair therefore have become of broader relevance to therapeutic interventions in human disease than the traditional narrow focus of intestinal disease.

To study intestinal epithelial regeneration, various mouse models have been developed. The most frequently used model induces intestinal epithelial injury by whole-body exposure to ionizing radiation.⁷ The response to irradiation has been well characterized in mice and is used to assess clonogenic capacity of intestinal epithelial stem cells.⁸ Radiation damage initiates a variety of cellular stress responses that result in widespread cell-cycle arrest and apoptosis, especially in rapidly proliferating stem cells in the intestinal crypts.⁹ A radiation dose of 14 Gy is sufficient to deplete most of the epithelial stem cells of the intestine and results in the loss of the majority of intestinal crypts, compromising mucosal integrity.^{9,10} This widespread epithelial damage rapidly induces a process of epithelial repair from surviving crypts. This regenerative response becomes morphologically apparent after approximately 72 hours with increased epithelial proliferation in hyperplastic surviving crypts and crypt multiplication through a process of fissioning and bifurcation.^{11,12}

Intestinal epithelial wounding and repair often has been studied *in vitro* using monolayers of colorectal cancer cells that are disrupted with the tip of a pipette, so-called *scratch assays*. The physiological relevance of these models, which perhaps depend more on epithelial cell migration by proliferating cancer cells than a stem cell-driven repair process, is unknown. Recently, *in vitro* culture methods have been developed that allow the generation and expansion of 3-dimensional intestinal organoids from primary intestinal epithelial cells.¹³ Organoids show all major hallmarks of the architecture of the intestinal epithelium, including crypt and villus domains and the presence of all epithelial cell lineages.¹³ With standard 3-dimensional culture conditions, organoids continuously are expanding in size and number of crypts, as such, they are sometimes believed to be more reflective of an epithelium in a state of repair than a truly homeostatic epithelial layer. The use of such organoids of primary epithelial cells in a model of damage and repair may provide a more physiological *in vitro* model than has been used previously. Such a model

may provide a platform to dissect the mechanisms that regulate epithelial repair and identify novel therapeutic targets.


Damage models using organoid culture exposed to irradiation have been developed previously, however, the recovery phase after induction of damage was not characterized extensively.^{14–17} Here, we performed a dose range of γ -radiation on intestinal epithelial organoids to identify a sublethal dose that results in a cycle of damage and repair, as measured by the loss and resurgence of expression of intestinal epithelial stem cell markers such as leucine-rich repeat-containing G-protein-coupled receptor 5 (*Lgr5*) and olfactomedin 4 (*Olfm4*), as well as morphologic characteristics. Transcriptomic analysis of different time points identified hepatocyte nuclear factor 4 α (HNF4 α) as one of the upstream regulators of the epithelial response to damage. *In vitro* experiments using *Hnf4a* mutant organoids, as well as *in vivo* experiments using epithelium-specific *Hnf4a* mutant mice, showed a critical role for HNF4 α in organoid expansion after seeding as well as epithelial repair after irradiation *in vivo*. Thus, we established a primary epithelial cell-based *in vitro* model of damage and repair that successfully identified a novel transcriptional regulator of epithelial repair.

Results

Irradiation-Induced Damage and Repair of Intestinal Organoids

To probe whether the regenerative response of the intestinal epithelium is maintained *in vitro*, we irradiated adult intestinal organoid cultures on day 3 after splitting. At this time point, organoids have established clear crypt-like buds. To titrate the optimal irradiation dose necessary to cause sublethal damage and subsequent repair, we exposed organoids to various doses of γ -radiation ranging from 1 to 10 Gy. Doses of irradiation less than 6 Gy did not visibly affect organoid growth. However, we noted a dose-dependent reduction in organoid survival starting at 6 Gy, and a complete organoid loss at 10 Gy. Moreover, at 6 Gy we observed initial loss of organoid buds with subsequent bud regeneration (Figure 1A and B). Based on these observations, we chose 6 Gy as the dose for further detailed analyses. We next analyzed the expression of stem cell markers *Lgr5* and *Olfm4* using quantitative reverse-transcription polymerase chain reaction (qRT-

Abbreviations used in this paper: BrdU, bromodeoxyuridine; EdU, 5-ethynyl-2'-deoxyuridine; ENR, epidermal growth factor, Noggin, and R-spondin; HNF4 α , hepatocyte nuclear factor 4 α ; IPA, ingenuity pathway analysis; Lgr5, leucine-rich repeat-containing G-protein-coupled receptor 5; Olfm4, olfactomedin 4; PBS, phosphate-buffered saline; qRT-PCR, quantitative reverse transcription polymerase chain reaction; TUNEL, terminal deoxynucleotidyl transferase-mediated deoxyuridine triphosphate nick-end labeling.

 Most current article

© 2020 The Authors. Published by Elsevier Inc. on behalf of the AGA Institute. This is an open access article under the CC BY-NC-ND license (<http://creativecommons.org/licenses/by-nc-nd/4.0/>).

2352-345X

<https://doi.org/10.1016/j.jcmgh.2020.02.007>

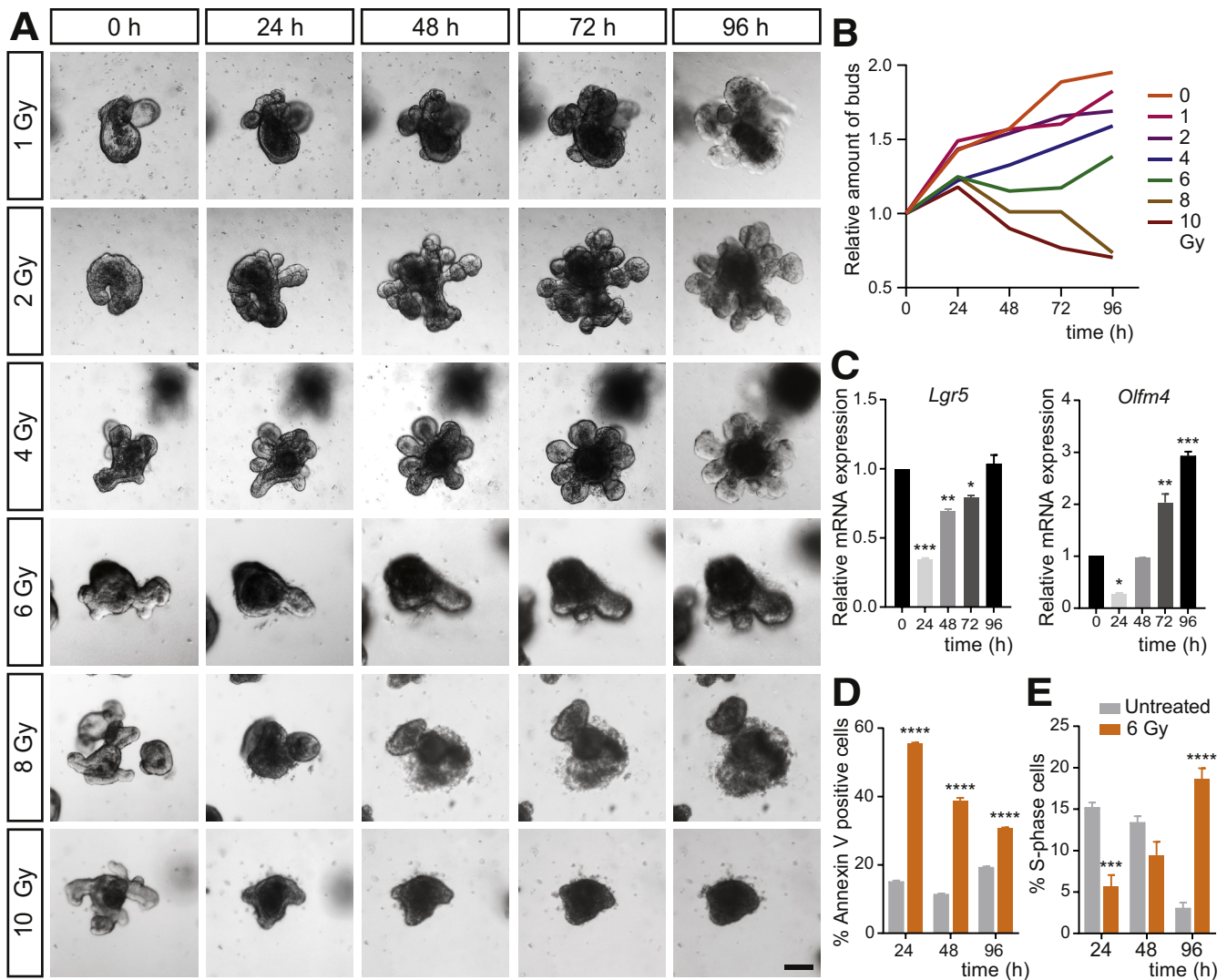


Figure 1. An in vitro model of intestinal damage and repair using 6 Gy irradiation on intestinal organoids. (A) Bright-field time series of intestinal organoids 24, 48, 72, and 96 hours after 0, 1, 2, 4, 6, 8, and 10 Gy γ -irradiation. Scale bar: 100 μ m. (B) Relative amount of buds at 0, 24, 48, 72, and 96 hours (compared with t = 0 hours) after 0, 1, 2, 4, 6, 8, and 10 Gy γ -irradiation. Representative of 2 independent experiments. Average of 44 organoids quantified per condition and time point. (C) Relative gene expression of stem cell markers *Lgr5* and *Olfm4* after 6 Gy irradiation compared with nonirradiated controls (n = 3). *Gapdh* is used as a reference gene. Data were obtained in 3 independent experiments and plotted as means \pm SEM. * P < .05, ** P < .01, and *** P < .001 compared with nonirradiated control calculated by 1-way analysis of variance. (D) Apoptosis and (E) cell proliferation assessment by means of Annexin V staining and EdU incorporation flow cytometry analysis (n = 3). Data are plotted as means \pm SEM. *** P < .001 and **** P < .0001 compared with nonirradiated time point-matched control calculated by 1-way analysis of variance. mRNA, messenger RNA.

PCR) at different time points after 6 Gy exposure. In line with the observed loss of organoid buds and subsequent regrowth, expression of both *Lgr5* and *Olfm4* was reduced significantly 24 hours after 6 Gy irradiation, and completely recovered at 96 hours for *Lgr5* (Figure 1C). Interestingly, expression levels of *Olfm4* increased to 3-fold greater than the expression at baseline (Figure 1C), similarly to what has been described in vivo.¹⁸

To further characterize the response to 6 Gy irradiation, we evaluated cell apoptosis and proliferation during the damage-repair process by flow cytometry analysis. Apoptosis was highest at 24 hours after irradiation and was

increased compared with the nonirradiated time point-matched control organoids at all time points, as assessed by both annexin V and propidium iodide staining (Figure 1D). On the other hand, the number of cells in S phase initially was reduced at 24 hours and then increased over time. At 96 hours after irradiation, proliferation was enhanced markedly, mirroring the timing of maximal epithelial proliferation observed after irradiation in vivo (Figure 1E). Together, these findings suggest that 6 Gy is a sufficient dose of irradiation to cause substantial damage in intestinal epithelial organoids, while retaining their regenerative potential. Moreover, we found that hallmarks of the

in vivo regenerative response were recapitulated in irradiated organoids in vitro.

Transcriptomic Analysis Identified HNF4 α as an Upstream Regulator of the Regenerative Response In Vitro

To investigate the transcriptional regulation of the regenerative epithelial response, we determined global gene expression changes by microarray analysis. As organoids undergo dynamic growth within the culture, we controlled each time point after irradiation to nonirradiated organoids grown in culture for the same time. Global expression profiling showed that the main transcriptional changes occurred at 24 and 48 hours after irradiation. At these time points we observed a clear separation of the irradiated cultures from matched nonirradiated cultures (Figure 2A and B). Remarkably, nonhierarchical clustering showed that the gene expression profile of the organoids at 96 hours after irradiation was highly similar transcriptionally to matched nonirradiated organoids, indicating almost complete organoid recovery within 96 hours (Figure 2B).

We subsequently used ingenuity pathway analysis (IPA), which showed that gene networks involved in apoptosis (P53-dependent), complement, inflammatory responses (eg, TNF- α signaling via NF- κ B), apical junction, tissue restitution, and remodeling (eg, epithelial-mesenchymal transition) were activated in irradiated organoids at 24 and 48 hours vs time point-matched nonirradiated controls (Figure 2C and D).

We then used IPA to determine the upstream regulators of cellular processes associated with the irradiation response in organoids. One of the main upstream regulators predicted by IPA was tumor protein 53 (P53), a key regulator of the DNA damage response to ionizing radiation, confirming the approach to identify upstream regulators (Figure 2E).¹⁹ In addition, other known regulators of radiation damage such as nuclear protein 1 (NUPR1), lysine-specific demethylase 5B (KDM5B), SMARCA4, and Forkhead box protein M1 (FOXM1) were on the list of upstream regulators.^{20–23} Besides these established transcriptional regulators of radiation damage, the analysis predicted transcription factor HNF4 α as one of the top upstream regulators of the response to irradiation (Figure 2E and F). Subsequent qRT-PCR analysis of organoid samples 24 hours after irradiation confirmed the expression changes of HNF4 α -regulated genes (Figure 2G). As previously described, HNF4 α is expressed mainly in the intestinal epithelium.²⁴ Together these results suggested that HNF4 α may be a novel regulator of epithelial repair.

HNF4 α Is Required for Organoid Establishment and Propagation In Vitro

To examine the functional role of HNF4 α in epithelial repair, we tried to isolate and culture intestinal epithelial cells from mice in which *Hnf4a* specifically was deleted from the intestinal epithelium, using a constitutively expressed epithelial Cre enzyme (*VillinCre*⁺*Hnf4a*^{f/f} mice) and littermate controls. Interestingly, we were unable to

generate organoids from *Hnf4a* mutant epithelium (Figure 3A). Because the seeding of isolated epithelial cells to form organoids mimics the process of damage and repair in many ways, this could fit well with a key role for HNF4 α in epithelial repair. To further examine this, we then isolated intestinal epithelial cells from mice in which an intestinal epithelium-specific Cre enzyme could be activated inducibly by treatment with tamoxifen (*VillinCre*⁺*ERT2*⁺*Hnf4a*^{f/f} mice) and used organoids from Cre-negative littermates as controls. Noninduced *VillinCre*⁺*ERT2*⁺*Hnf4a*^{f/f} grew similar to controls. However, similar to epithelial cells derived from the constitutive *Hnf4a* mutant epithelium, inducible deletion of *Hnf4a* upon exposure to tamoxifen resulted in a failure to propagate organoids in culture, whereas growth of Cre-negative organoids exposed to tamoxifen was unremarkable (Figure 3B, upper panel). These results suggest that HNF4 α plays a vital role in establishing organoids from clusters of broken up epithelial cells in the process of organoid damage and reseeding during organoid passaging.

We next attempted to rescue tamoxifen-treated *Hnf4a*-deficient organoids by supplementing medium with Wnt3A-conditioned medium, which promotes intestinal stem cell survival.²⁵ One day after Cre induction, the medium in all groups was refreshed with either standard medium containing epidermal growth factor, Noggin, and R-spondin (ENR), or ENR supplemented with Wnt3A (Figure 3B, lower panel). At 7 days after induction, only 50% of the *Hnf4a*-deficient organoids survived without supplementation of Wnt3A (Figure 3C). Surviving organoids appeared to have more cell death and debris in their lumen than *Hnf4a*-expressing control organoids (Figure 3B). On the other hand, when the organoid medium was supplemented with Wnt3A, almost all *Hnf4a*-deficient organoids were able to survive with a similar proliferation rate compared with controls (Figure 3C). However, when they subsequently were passaged, the *Hnf4a*-deficient organoids showed a drastic decrease in viability that could not be recovered by Wnt3A supplementation (Figure 3D). Perhaps supplementation with other growth factors could increase viability of *Hnf4a* knockout organoids at subsequent passages. In conclusion, although Wnt3A supplementation partially can rescue established organoids in which *Hnf4a* is deleted, this is insufficient to rescue epithelial cell death after passaging. These experiments establish a key role for HNF4 α during organoid establishment and in organoid regeneration after passaging.

HNF4 α Is Required for Intestinal Epithelial Regeneration In Vivo

To study the role of HNF4 α in intestinal regeneration in vivo, we examined epithelial repopulation after irradiation in mice in which *Hnf4a* was deleted in the intestinal epithelium (*VillinCreERT2*⁺*Hnf4a*^{f/f}) using injections with tamoxifen and in tamoxifen-treated Cre-negative littermate control mice (*VillinCreERT2*⁻*Hnf4a*^{f/f}). All mice received 14 Gy whole-body irradiation and were euthanized after 96 hours (Figure 4A). Recombination efficiency was assessed

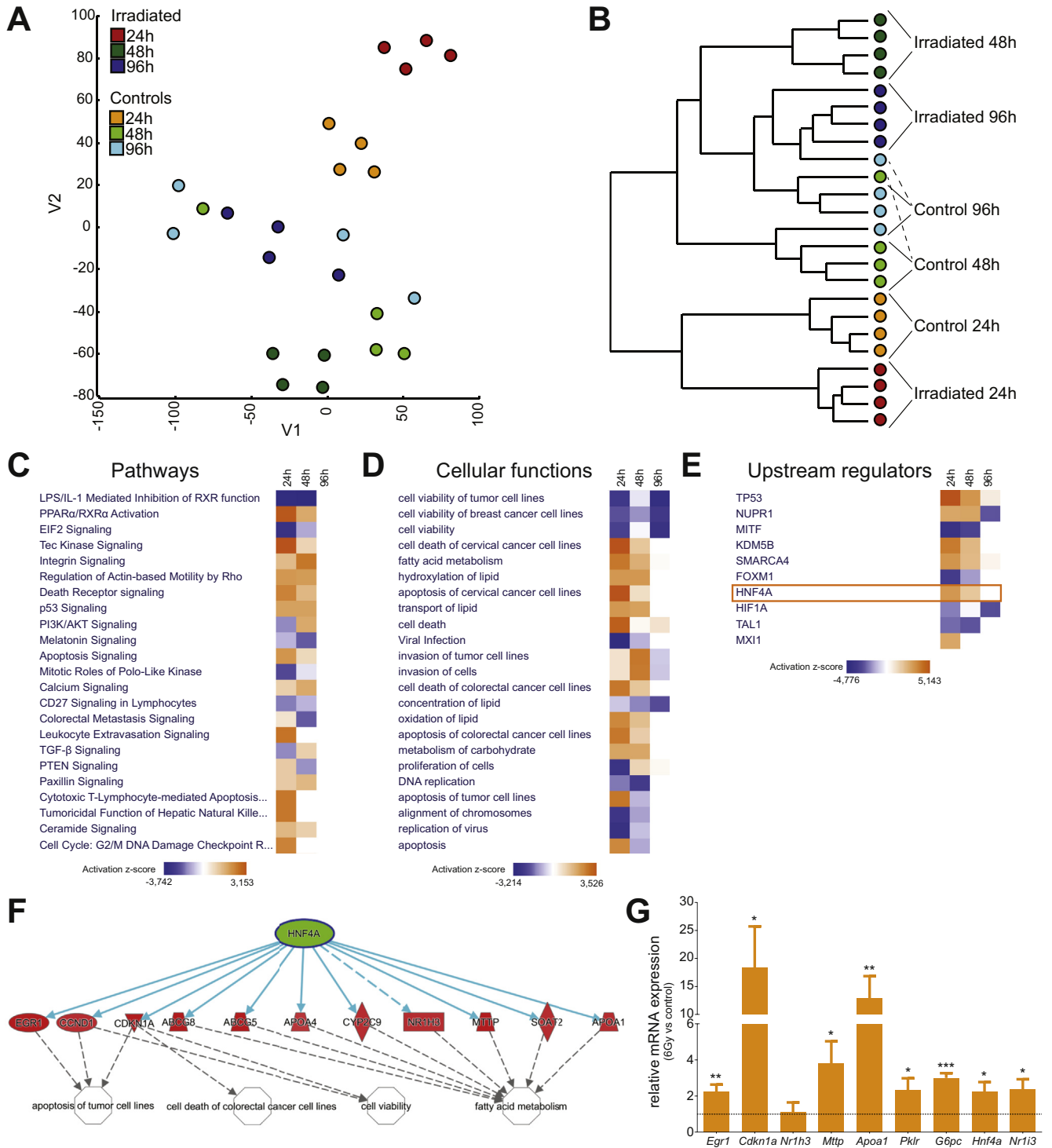


Figure 2. Gene expression array identifies HNF4 α as a potential upstream regulator of intestinal repair. (A) T-distributed stochastic neighbor embedding plot and (B) hierarchical clustering analysis of gene expression data from irradiated and time point-matched nonirradiated intestinal organoids at 24, 48, and 96 hours after 6 Gy irradiation (n = 4). (C) Differentially regulated pathways, (D) cellular functions, and (E) regulating transcription factors as determined by Ingenuity pathway analysis (IPA). (F) Predicted HNF4 α target genes in organoids at 24 hours after 6 Gy irradiation from IPA. (G) Differential expression of HNF4 α target genes was confirmed by qRT-PCR. Bars represent relative messenger RNA (mRNA) expression of organoids at 24 hours after irradiation compared with nonirradiated organoids (n = 3). Data were obtained from 3 independent experiments and plotted as means \pm SEM. * P < .05, ** P < .01, and *** P < .001 as calculated by the Student t test. IL, interleukin; LPS, lipopolysaccharide; TGF, transforming growth factor.

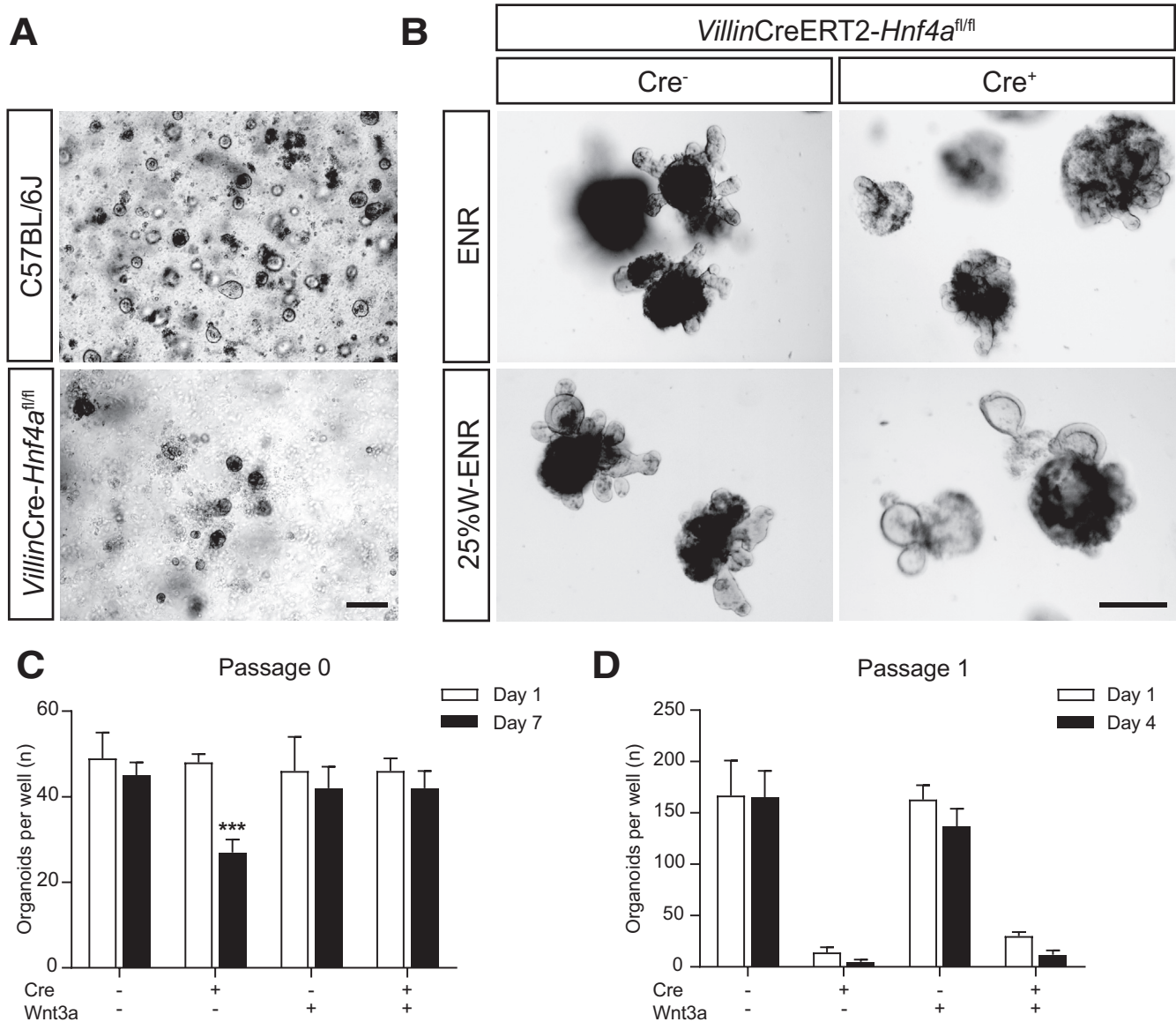


Figure 3. HNF4 α is essential for intestinal organoid growth. (A) Bright-field microscopic images of wild-type and *VillinCre-Hnf4a^{fl/fl}* small-intestinal crypts and (B) tamoxifen-induced *VillinCreERT2⁻-Hnf4a^{fl/fl}* and *VillinCreERT2⁺-Hnf4a^{fl/fl}* organoids 6 days after tamoxifen induction with and without Wnt3A supplementation. Representative images are shown. Scale bars: 250 μ m. (C) Quantification of the amount of organoids in tamoxifen-inducible *Hnf4a* mutant organoids with and without Wnt3A supplementation at 1 and 7 days after tamoxifen treatment (n = 4). (D) Organoids were passaged 7 days after tamoxifen treatment, and the amount of surviving organoids was quantified on days 1 and 4 after passaging (n = 4). Data are plotted as means \pm SEM. ****P* < .001 as calculated by 2-way analysis of variance. Representative images are shown. W-ENR, epidermal growth factor, Noggin, and R-spondin supplemented with Wnt3A.

by HNF4 α immunohistochemistry and showed complete absence of HNF4 α protein in the epithelial layer of tamoxifen-treated *VillinCreERT2⁺Hnf4a^{fl/fl}* mice (Figure 4B). Between 48 and 96 hours after irradiation, the intestinal epithelium was in a regenerative state, characterized by enlarged hyperproliferative crypts (Figure 4C, left panel). We observed that the control animals showed a significantly higher amount of hyperproliferative crypts compared with *Hnf4a*-deficient animals (Figure 4C and D). When the number of proliferating cells was examined using immunohistochemistry for bromodeoxyuridine

(BrdU), we also observed that the number of proliferating cells per surviving crypt was reduced substantially versus the number of proliferating cells in surviving wild-type crypts (Figure 4E and F). Quantification of apoptotic cells by terminal deoxynucleotidyl transferase-mediated deoxyuridine triphosphate nick-end labeling (TUNEL) staining did not show a difference in the overall number of apoptotic cells (Figure 4G and H). Together these data suggest that HNF4 α plays an important role in crypt survival and proliferating cell survival after irradiation in vivo.

We examined the expression of stem cell markers *Lgr5* and *Olfm4* using either in situ hybridization or qRT-PCR. We did not observe any difference in *Lgr5* expression between control and *Hnf4a*-deficient animals using either in situ hybridization or qPCR (Figure 5A and B). Interestingly, *Olfm4* expression was abrogated almost completely in *Hnf4a*-deficient animals versus controls after irradiation ($P < .001$) (Figure 5C and D). Taken together, our data suggest that the role of HNF4 α in epithelial regeneration may not be associated with survival and proliferation of classic *Lgr5*-positive crypt base columnar cells. Given the clear reduction in the number of surviving crypts and BrdU-positive cells in *Hnf4a* mutant animals, this may mean that HNF4 α acts at the level of the progenitor cells, which have lost expression of crypt base columnar stem cell markers and cycle very rapidly for a number of cycles until the cells commit to final differentiation.

Increased Secretory Lineage Differentiation in *Hnf4a*-Deficient Epithelium

We next examined the effect of the loss of HNF4 α on epithelial cell differentiation during the repair process after irradiation. We observed an increased differentiation toward the secretory lineages in *Hnf4a* mutant epithelium as previously described.^{26,27} Periodic acid–Schiff staining showed increased numbers of goblet cells in mutant animals versus controls (Figure 6A and B). This correlated with increased expression of *Muc2*, the major mucin expressed by goblet cells (Figure 6C). Immunohistochemistry for the Paneth cell marker lysozyme showed an increased number of Paneth cells (Figure 6D and E). Indeed, gene expression of the Paneth cell-associated Defensin *Defcr1* was increased in *Hnf4a*-deficient animals (Figure 6F). Consistently, expression of sex-determining region Y-box 9 (*Sox9*), a transcription factor associated with Paneth cell differentiation,²⁸ was increased in *Hnf4a*-deficient animals (Figure 6G and H). Thus, the role of HNF4 α in restricting secretory lineage differentiation is conserved between homeostasis and epithelial repair.

Impaired Regeneration in *Hnf4a*^{-/-} Mice Is Associated With Altered Metabolism

To further investigate the inability of *Hnf4a*-deficient mice to regenerate upon irradiation, we performed genome-wide gene expression analyses on jejunal tissue samples from irradiated *VillinCreERT2*⁺*Hnf4a*^{fl/fl} *Hnf4a* mutant and control *VillinCreERT2*⁻*Hnf4a*^{fl/fl} control mice. A principal component analysis showed that the 2 genotypes separated across principal component 1 indicated a different response to irradiation (Figure 7A). Interestingly, the jejunal tissue of nonirradiated *Hnf4a*-deficient mice showed no significant alterations in the transcriptional profile compared with nonirradiated wild-type mice (GSE11759). To assess differences between irradiated *Hnf4a*-deficient and control mice, we performed differential gene expression analysis that showed 778 differentially expressed genes (483 up-regulated, 295 down-regulated; fold change >1.5; analysis of variance $P < .05$). Among the top 50 up-regulated and

down-regulated genes were *Hnf4a*, *Olfm4*, and *Cldn15*, which is an established target of HNF4 α (Figure 7B).²⁹ IPA of the genes that were expressed differentially between irradiated *VillinCreERT2*⁺*Hnf4a*^{fl/fl} mutant mice and *VillinCreERT2*⁻*Hnf4a*^{fl/fl} controls showed significant changes in pathways related to amino acid and lipid metabolism (Figure 7C). These analyses may suggest that the intestine of irradiated *Hnf4a*-deficient mice is unable to sustain the high metabolic demands of the regeneration process.

Discussion

There are currently no useful in vitro models of intestinal epithelial damage and repair that use primary epithelial cells. An organoid model of irradiation-induced epithelial damage and repair was used previously,^{14–17} however, a careful transcriptional analysis of the repair process has not been performed previously. Here, we describe a model of epithelial regeneration using sublethally irradiated small-intestinal organoids that recapitulates key aspects of epithelial repair after irradiation in vivo. Regeneration is slightly accelerated in organoid culture, with irradiated organoids clustering transcriptionally with time-matched controls after only 96 hours when epithelial repair is still fully ongoing in vivo.³⁰ This difference may well be related to the presence of luminal content and microbiota and/or, for example, lamina propria (inflammatory) cell types that may alter the epithelial repair process in vivo.³¹ Our transcriptional analysis of organoids at different stages of repair identified several established transcriptional regulators of the response to irradiation. HNF4 α was identified as a potential novel upstream driver of a damage response program. Our subsequent functional in vitro and in vivo experiments confirmed a clear role for HNF4 α in epithelial repair. The fact that *Hnf4a* mutant epithelial cells failed to generate organoids and that organoids in which *Hnf4a* was inducibly deleted failed to propagate in vitro suggests that HNF4 α plays a role in epithelial regeneration well beyond damage induced by irradiation.

Interestingly, HNF4A has been identified as an ulcerative colitis risk gene in human beings.³² Mice, in which *Hnf4a* is deleted from the epithelium, are more susceptible to chemically induced colitis,²⁴ and gradually develop spontaneous ulcerative colitis-like disease as they age.²⁹ Although the mechanisms of the damage induced in colitis and irradiation are different, the effects of loss of *Hnf4a* on the regenerative response might be similar. HNF4 α has been shown to contribute to epithelial barrier function by regulating epithelial tight junctions, which could be an important contributing factor for the development of colitis in mice.^{29,33} However, epithelial barrier function is less likely to account for the phenotype we observed in our irradiation experiments. HNF4 α was not required for *Lgr5* expression or maintenance of *Lgr5*⁺ cells as judged by in situ hybridization. The profound effect of loss of HNF4 α on epithelial repair therefore likely is not linked to *Lgr5*⁺ stem cell survival. On the contrary, the effect on *Olfm4*, which is expressed more broadly than the stem cell compartment, is profound. The molecular function of *Olfm4* is not well

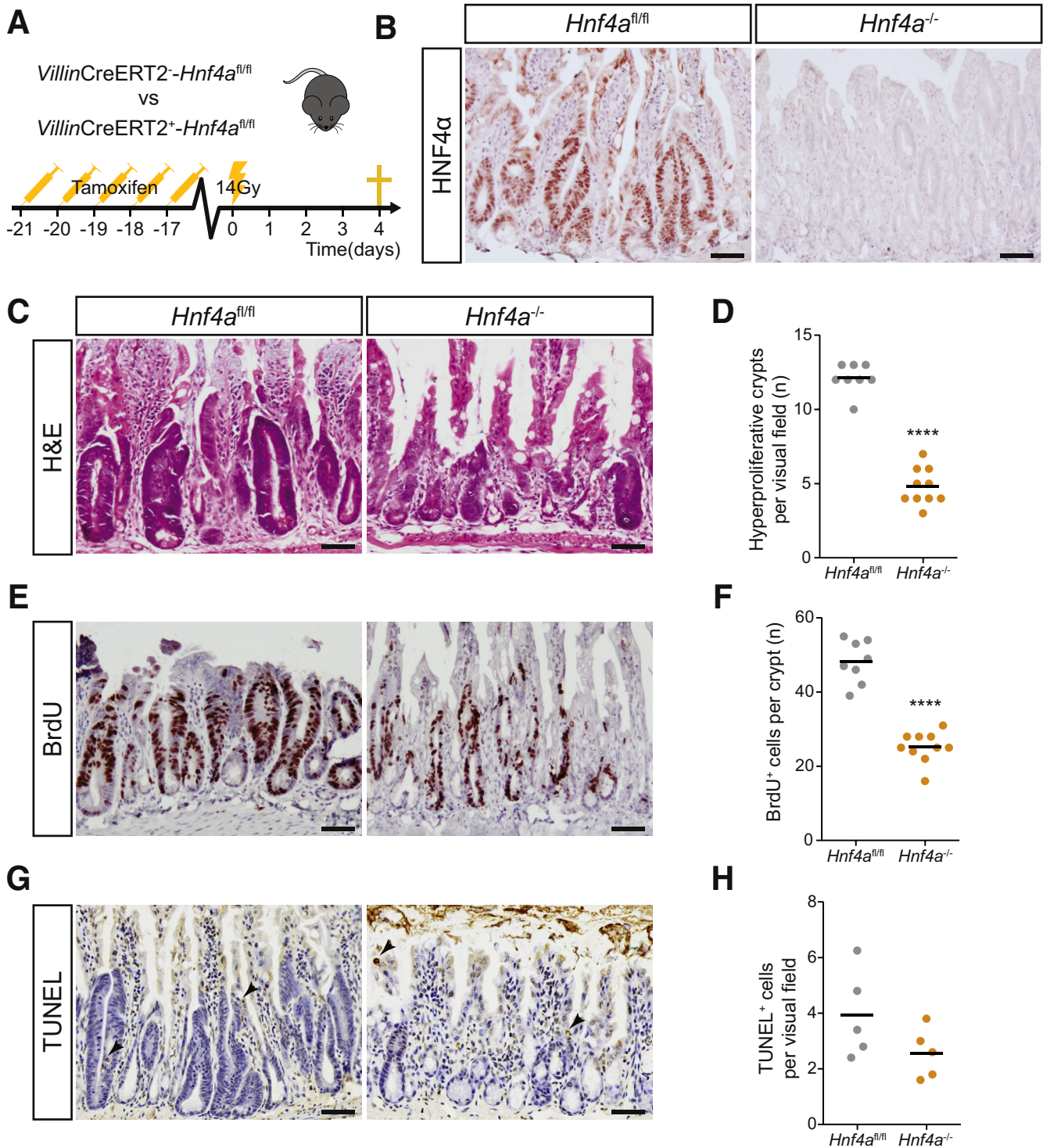


Figure 4. HNF4 α is required for epithelial regeneration after irradiation in vivo. (A) Schematic overview of the mouse model: VillinCreERT2⁻-Hnf4a^{fl/fl} and VillinCreERT2⁺-Hnf4a^{fl/fl} mice were injected with tamoxifen for 5 consecutive days. One week after the final injection, both groups received 14 Gy whole-body irradiation and were killed 96 hours after treatment (n = 8 and 10 per group). (B) Immunostaining for HNF4 α in small-intestinal tissue at 96 hours after irradiation. (C) H&E of small-intestinal tissue at 96 hours after irradiation. (D) Quantification of hyperproliferative crypts per visual field. (E) BrdU staining of small-intestinal tissue at 96 hours after irradiation. (F) Quantification of BrdU-positive cells per crypt. (G) TUNEL staining in small-intestinal tissue at 96 hours after irradiation. (H) Quantification of TUNEL-positive cells per visual field. n = 8 and 10 per group. Mean values are shown, 1 dot represents 1 mouse. ****P < .0001 as calculated by the Student t test. Slides were counterstained with hematoxylin. Scale bars: 50 μ m. Representative images are shown.

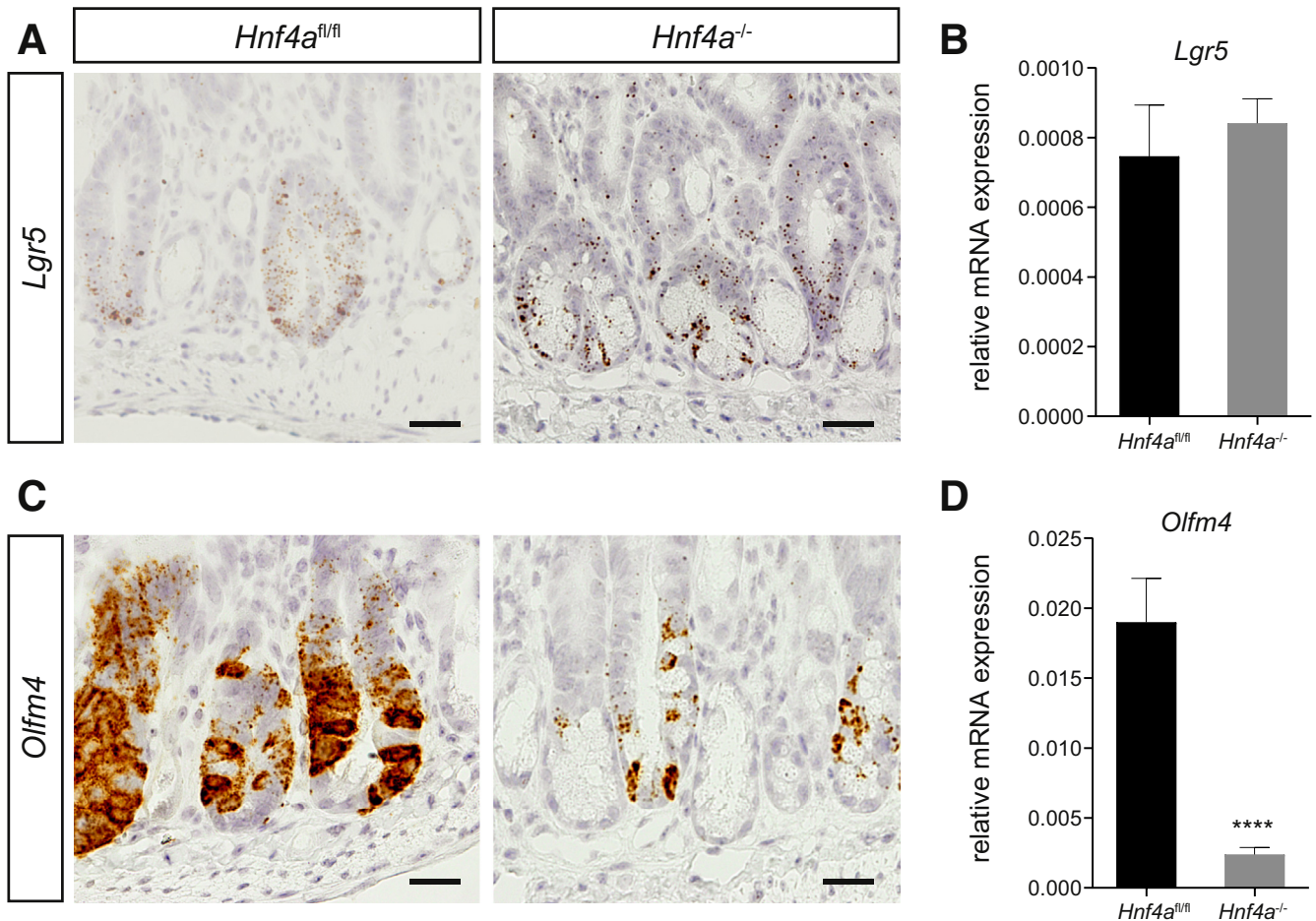


Figure 5. *Olfm4* is nearly abolished in *Hnf4a*-deficient intestinal regeneration. (A) RNAscope in situ hybridization of *Lgr5* in *VillinCreERT2*⁻-*Hnf4a*^{fl/fl} and *VillinCreERT2*⁺-*Hnf4a*^{fl/fl} mice at 96 hours after irradiation in small-intestinal tissue. (B) qRT-PCR of *Lgr5* in small-intestinal tissue. (C) RNAscope in situ hybridization of *Olfm4* in *VillinCreERT2*⁻-*Hnf4a*^{fl/fl} and *VillinCreERT2*⁺-*Hnf4a*^{fl/fl} mice at 96 hours after irradiation in small-intestinal tissue. Scale bars: 25 μ m. (D) qRT-PCR of *Olfm4* in small-intestinal tissue. *Gapdh* is used as a reference gene. n = 8 and 10 per group. Data are plotted as means \pm SEM. *****P* < .0001 as calculated by the Student *t* test. Slides were counterstained with hematoxylin. Representative images are shown. mRNA, messenger RNA.

understood, but it appears to affect a diverse set of cellular processes, including proliferation, differentiation, apoptosis, adhesion, and innate immunity against bacterial infection.^{34,35} It has been described previously that *Hnf4a*-deficient mice have a higher cell proliferation rate,²⁶ and dividing cells are more susceptible to irradiation damage. This proliferative state could explain part of the phenotype we observed. Based on analyses of differently expressed genes between irradiated *Hnf4a*-deficient and control mice, genes downstream of HNF4 α are affected. Amino acid metabolism and lipid metabolism were among the most affected pathways in the mutant mice. This could be related to the observed regenerative failure in *Hnf4a*-deficient mice. These pathways are pivotal for cellular growth and regeneration upon damage. However, further experiments will be required to address this possibility. Identifying key mediators of regeneration is crucial to determine therapeutic approaches promoting intestinal epithelial regeneration after injury. It should be noted that HNF4 α has been shown to bind to approximately 20,000 loci in the mouse genome,³⁶

affecting target genes that regulate cellular metabolism, function, and differentiation. Therefore, it is likely that multiple mechanisms govern the regenerative response downstream of HNF4 α .

Small-molecule inhibitors for HNF4 α currently are being investigated,^{37–39} mostly for cancer therapy. If these drugs will be used in clinical trials, our data suggest that caution should be taken when combination therapy with radiotherapy is considered.

Methods

Animals

All animal experiments were performed in accordance with the Animal Ethical Committee guidelines of the Academic Medical Center of Amsterdam, The Netherlands (permit ALC102556). A tamoxifen-inducible and intestinal epithelium-specific knockout of *Hnf4a* was obtained by mating *Hnf4a*^{fl/fl} mice and *VillinCreERT2* mice, both on a C57BL/6 background, as previously described.^{27,40} For all

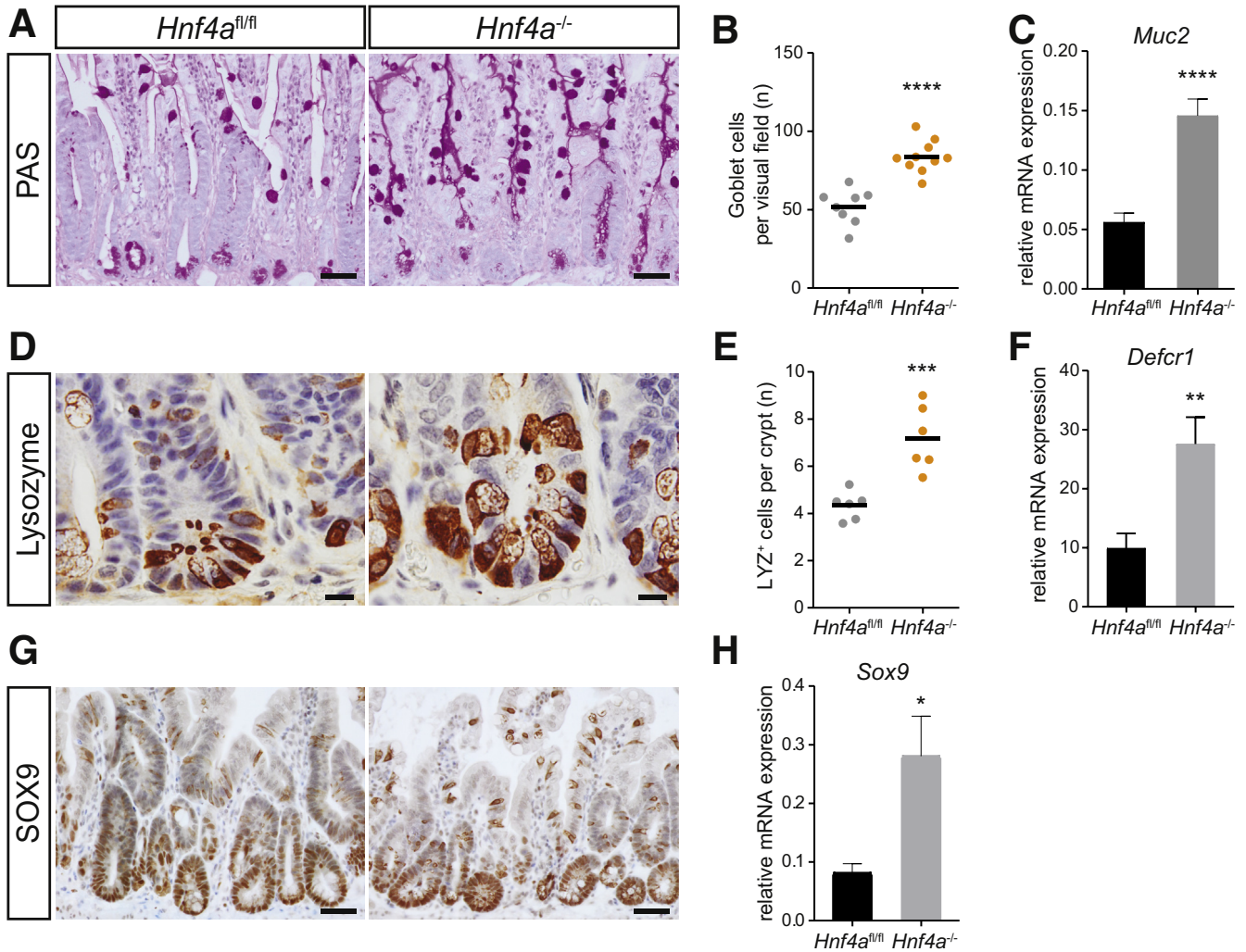


Figure 6. *Hnf4a*-deficient intestinal regeneration leads to increased differentiation into the secretory lineage. (A) Periodic acid–Schiff (PAS) staining of *VillinCreERT2⁻-Hnf4a^{fl/fl}* and *VillinCreERT2⁺-Hnf4a^{fl/fl}* mice at 96 hours after irradiation in small-intestinal tissue. (B) Quantification of goblet cells per visual field. (C) qRT-PCR of *Muc2* in small-intestinal tissue. (D) Lysozyme immunostaining of *VillinCreERT2⁻-Hnf4a^{fl/fl}* and *VillinCreERT2⁺-Hnf4a^{fl/fl}* mice at 96 hours after irradiation in small-intestinal tissue. (E) Quantification of lysozyme-positive cells per crypt. (F) qRT-PCR of *Defcr1* in small-intestinal tissue. (G) SOX9 immunostaining of *VillinCreERT2⁻-Hnf4a^{fl/fl}* and *VillinCreERT2⁺-Hnf4a^{fl/fl}* mice at 96 hours after irradiation in small-intestinal tissue. (H) qRT-PCR of *Sox9* in small-intestinal tissue. *Gapdh* is used as a reference gene. n = 8 and 10 per group. (B and E) Data are plotted as means, 1 dot represents 1 mouse, or as means ± SEM. **P* < .05, ***P* < .01, ****P* < .001, and *****P* < .0001 as calculated by the Student *t* test. Slides were counterstained with hematoxylin. Scale bars: (A and G) 50 μm, and (D) 10 μm. Representative images are shown. mRNA, messenger RNA.

experiments, solely male mice were used and littermates were used as controls. For the CreERT2-mediated recombination, mice were given 1 mg tamoxifen (Sigma, St Louis, MO) administered by oral gavage for 5 consecutive days. After 3 weeks, the animals were treated with 14 Gy whole-body γ -irradiation and euthanized 96 hours afterward. Two hours before death all mice received an intraperitoneal injection of 100 mg/kg BrdU (10 mg/mL in phosphate-buffered saline [PBS]; Sigma-Aldrich, St Louis, MO). After death, the intestines were harvested, washed with cold PBS, and sectioned into mid, distal, and proximal tissue of the small intestine. For further analysis, the tissues were either snap-frozen or 4% formalin-fixed and embedded in paraffin.

Mouse Intestinal–Crypt Isolation and Organoid Culture

Small-intestinal single crypts were isolated from C57BL/6, *VillinCre-Hnf4a^{fl/fl}* and *VillinCreERT2-Hnf4a^{fl/fl}* mice and cultured in Matrigel (BD Biosciences, Franklin Lakes, NJ). Harvesting and expansion of intestinal organoids was performed as described previously.¹³ In brief: crypts were harvested by incubating opened small intestines in PBS containing 2 mmol/L EDTA. The epithelium was released by vigorous shaking and crypts were separated using a 70-μm cell strainer. Single crypts were cultured in ENR medium, containing Advanced Dulbecco's modified Eagle medium (Invitrogen/Thermo Fisher, Waltham, MA) supplemented

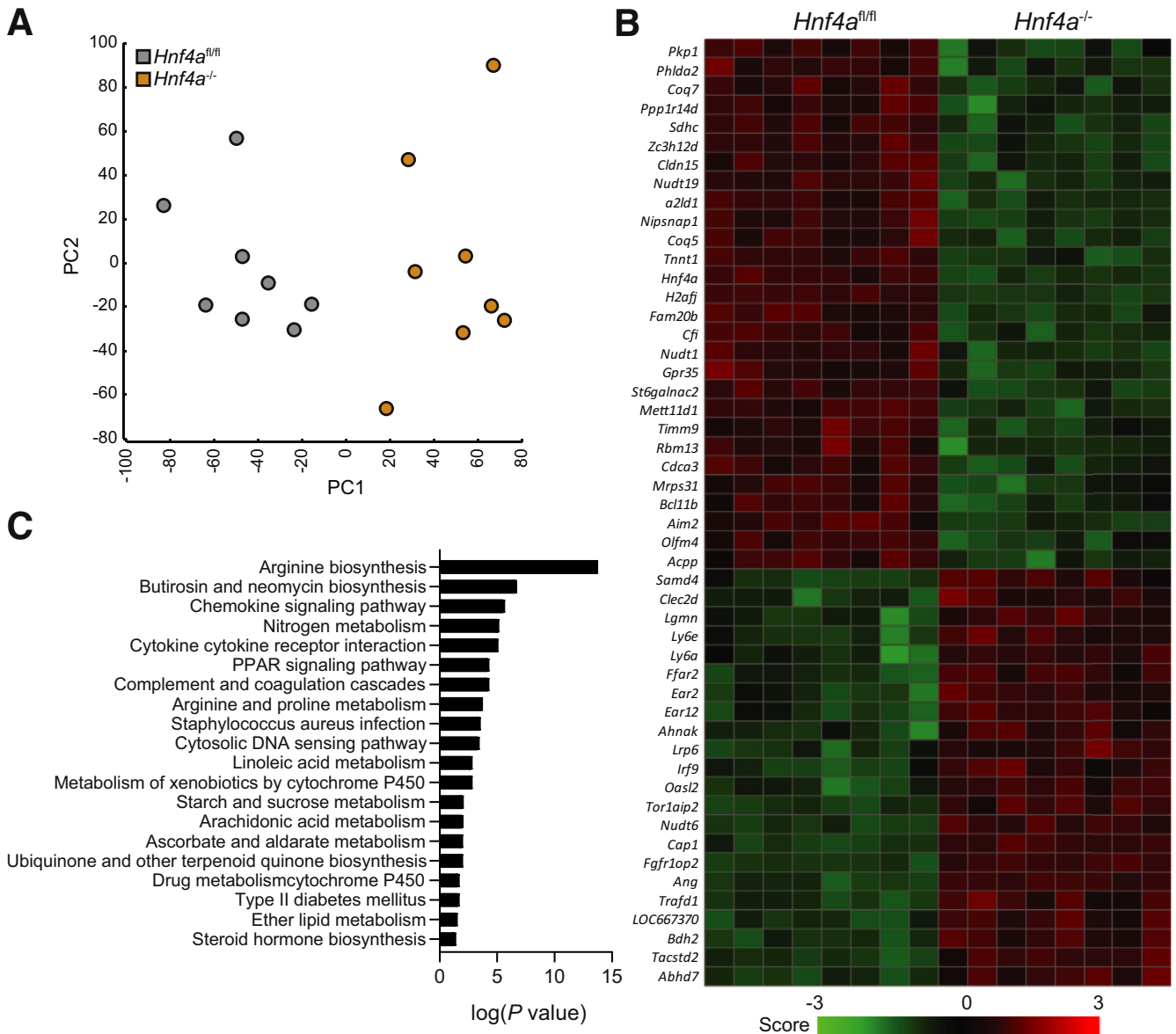


Figure 7. Metabolic pathways are affected in regenerating *Hnf4a* knockout mice. (A) Principal component analysis of microarray data from small-intestinal tissue of *VillinCreERT2*⁻-*Hnf4a*^{fl/fl} and *VillinCreERT2*⁺-*Hnf4a*^{fl/fl} mice 96 hours after irradiation. (B) Heatmap showing the top 50 up-regulated and down-regulated genes from the microarray. (C) Log(P value) of pathway analysis (KEGG pathways). *n* = 8 per group. KEGG, Kyoto Encyclopedia of Genes and Genomes; PC, principal component.

with 1% penicillin/streptomycin, 1% HEPES buffer, 1% GlutaMAX, 50 ng/mL epidermal growth factor, 20% Noggin-conditioned medium, 10% R-spondin-conditioned medium, 1 \times B-27 supplement, 1 \times N-2 supplement (all from Invitrogen), and 1.25 mmol/L *n*-acetyl cysteine (Sigma). The organoids then were passaged weekly by mechanical disruption in a splitting ratio of 1:3 or 1:4. Cre-mediated recombination of *Hnf4a* in organoids was established by adding 1 μ g/mL tamoxifen to the culture medium for 24 hours. Subsequently, the medium with tamoxifen was removed and replaced by standard ENR medium or ENR medium supplemented with 25% WNT3A conditioned medium.

For the in vitro irradiation-induced damage experiments, we treated the organoid cultures 3 days after seeding with various doses of γ -radiation ranging between 1 and 10 Gy. Microscopic bright-field images were captured with a Leica DMi8 microscope (Leica, Wetzlar, Germany).

RNA Extraction, qRT-PCR, and Microarray Analysis

RNA was extracted from the organoids using the Isolate II RNA Mini Kit (Bioline, London, United Kingdom) following the manufacturer's instructions. The intestinal tissue RNA was extracted with TRI Reagent (Sigma-Aldrich) and RNA clean-up

Table 1. qPCR Primer Sequences

Gene	Forward	Reverse
<i>Apoa1</i>	GAACGAGTACCACACCAGGG	ATGGGCATCAGACTATGGCG
<i>Cdkn1a</i>	TCCACAGCGATATCCAGACA	GGACATCACCAGGATTGGAC
<i>Defcr1</i>	TCAAGAGGCTGCAAAGGAAGA	ACCCTTTCTGCAGGTTCCATT
<i>Egr1</i>	GAGTCGTTTGGCTGGGATAA	CCTTCAATCCTCAAGGGGAG
<i>G6pc</i>	CAGTGGTCGGAGACTGGTTC	AGATGACGTTCAAACACCGGA
<i>Hnf4a</i>	AAATGTGCAGGTGTTGACCA	CTCACGCTCCTCCTGAAGAA
<i>Lgr5</i>	TGTGTCAAAGCATTTCACGC	CAGCGTCTTCACCTCCTACC
<i>Mttp</i>	CCAGGACCTCACTGCTTCTT	GCCAGTTGTGTGACCGCTA
<i>Muc2</i>	GAAGCCAGATCCCGAAACCA	GAATCGGTAGACATCGCCGT
<i>Nr1h3</i>	GGGAAACGCGACAGTTTTGG	ACTCCGTTGCAGAATCAGGA
<i>Nr1i3</i>	GGAGCGGCTGTGGAAATATTGCAT	TCCATCTGTAGCAAAGAGGCCCA
<i>Olfm4</i>	AACATCACCCAGGCTACAG	TGTCCACAGACCCAGTGAAA
<i>Pklr</i>	CAGTATGGAAGGGCCAGCAG	TGGGAGAAGTTGAGTCGTGC
<i>Sox9</i>	AGGAAGCTGGCAGACCAGTA	CTCCTCCACGAAGGGTCTCT

was performed with the RNeasy kit (Qiagen, Hilden, Germany) following the manufacturer's instructions. The qRT-PCR was performed using SybrGreen (Roche, Basel, Switzerland) according to the manufacturer's protocol on a Bio-Rad iCycler (Bio-Rad, Hercules, CA). The primer sequences used are shown in Table 1.

To confirm the knockout of *Hnf4a* after tamoxifen induction, a qRT-PCR was performed using primers located in exons 4 and 5, as well as exons 3 and 5, as described by Cattin et al.²⁷

For the microarrays, RNA was amplified using a Total-Prep RNA amplification kit for Illumina (Illumina, San Diego, CA), and labeled using a complementary RNA labeling kit for Illumina Arrays (Illumina), followed by hybridization with Illumina Ref8 v2.0 mouse slides. Expression profiles were deposited in the following GEO repositories: GSE141515 (organoid irradiation) and GSE141518 (*Hnf4a* knockout irradiation). Initial normalization was performed using Genome studio software (v2.0; Illumina). Further analysis was performed with the R2 Bioinformatic platform (<http://r2.amc.nl>; AMC, Amsterdam, The Netherlands), and IPA software (version 2.4; Qiagen).

Immunohistochemistry and TUNEL Staining

For histology, sections (5 μ m) were deparaffinized with xylene and rehydrated in a graded series of ethanol.

For periodic acid-Schiff staining, slides were incubated for 30 minutes in 0.5% periodic acid and for 30 minutes in Schiff's solution (VWR Chemicals, Radnor, PA).

For immunohistochemistry, endogenous peroxidase activity was blocked with 3% H₂O₂ in PBS. For antigen retrieval, tissue was cooked in 0.01 mol/L sodium citrate solution (pH 6.0) for 20 minutes or alternatively in 0.1 mol/L sodium EDTA (pH 9.0) for 20 minutes. Nonspecific binding was prevented by incubation with an avidin and biotin blocking solution (Vector Laboratories, Burlingame, CA). Tissues sections were incubated overnight with a primary antibody. Subsequently, the sections were incubated with a

biotinylated secondary antibody for 10 minutes, followed by a 10 minutes incubation with a LSAB2 streptavidin-horseradish peroxidase (K1016; DAKO, Agilent, Santa Clara, CA), and horseradish peroxidase detection with Vector NovaRED substrate (SK-4800; Brunschwig, Amsterdam, The Netherlands). Mayer's hematoxylin (Sigma-Aldrich) was used as nuclear counterstain. The following antibodies were used: anti-HNF4 α (sc-6556; Santa Cruz Biotechnology, Dallas, TX), mouse anti-BrdU (BMC9318; Roche), rabbit anti-activated caspase 3 (9661S; Cell Signaling Technology, Danvers, MA), rabbit antilysozyme (A0099; DAKO), and rabbit anti-SOX9 (AB5535; Millipore, Burlington, MA).

For TUNEL staining, the in situ cell death detection kit from Roche was used (reference number: 11684 817 910) according to the manufacturer's instructions.

Images were captured with an Olympus BX51 (Olympus, Tokyo, Japan) microscope.

In Situ Hybridization

RNAscope in situ hybridization (Advanced Cell Diagnostics, Biotechnne, Newark, CA) was performed according to the Formalin-Fixed Paraffin-Embedded Sample Preparation and Pretreatment for RNAscope 2.5 assay and RNAscope 2.5 HD Detection Reagent-RED protocols provided by the manufacturer. In brief, slides were deparaffinized, treated with heat antigen retrieval and protease, followed by a series of hybridizations with the target-specific probes and amplifiers. All components from the protocol were provided in RNAscope pretreatment reagents (322300 and 322000) and RNAscope 2.5 HD detection reagent (322350). The following probes were used: mm_*Olfm4* (311831) and mm_*Lgr5* (312171).

Flow Cytometry

For analysis of apoptosis, small-intestinal organoids were fixed and stained with anti-Annexin V-fluorescein

isothiocyanate (560534; BD Pharmingen, Franklin Lakes, NJ). Expression was analyzed by flow cytometry using a FACS Fortessa (BD Bioscience Franklin Lakes, NJ) with FlowJo software (Treestar, Inc, Ashland, OR). For analysis of proliferation, small-intestinal organoids were incubated with 10 mmol/L 5-ethynyl-2'-deoxyuridine (EdU) for 2 hours at 37°C. Subsequently, we used the Click-iT EdU Alexa Fluor 647 Flow Cytometry Assay Kit (ThermoFisher Scientific) according to the manufacturer's manual. Cells were double-stained with propidium iodide to determine the cell-cycle phase. EdU-positive (S-phase) cells were quantified by flow cytometry on dissociated organoid cultures using a FACS Fortessa (BD Bioscience) with FlowJo software (Treestar, Inc). Dead cells were excluded with propidium iodide.

Statistical Analysis

Data are presented as means and SEM. The Student *t* test was used to analyze data with 2 groups. One-way analysis of variance with the Tukey multiple comparison test was performed for data with more than 2 groups. For statistical analysis, GraphPad Prism (version 7; GraphPad Software, Inc, La Jolla, CA) was used. A *P* value less than .05 was considered statistically significant.

All authors had access to the study data and reviewed and approved the final manuscript.

References

1. Cliffe LJ, Humphreys NE, Lane TE, Potten CS, Booth C, Grecnis RK. Accelerated intestinal epithelial cell turnover: a new mechanism of parasite expulsion. *Science* 2005; 308:1463–1465.
2. Heijmans J, van Lidth de Jeude JF, Koo BK, Rosekrans SL, Wielenga MC, van de Wetering M, Ferrante M, Lee AS, Onderwater JJ, Paton JC, Paton AW, Mommaas AM, Kodach LL, Hardwick JC, Hommes DW, Clevers H, Muncan V, van den Brink GR. ER stress causes rapid loss of intestinal epithelial stemness through activation of the unfolded protein response. *Cell Rep* 2013;3:1128–1139.
3. Matthews JR, Sansom OJ, Clarke AR. Absolute requirement for STAT3 function in small-intestine crypt stem cell survival. *Cell Death Differ* 2011;18:1934–1943.
4. Rahman K, Desai C, Iyer SS, Thorn NE, Kumar P, Liu Y, Smith T, Neish AS, Li H, Tan S, Wu P, Liu X, Yu Y, Farris AB, Nusrat A, Parkos CA, Anania FA. Loss of junctional adhesion molecule a promotes severe steatohepatitis in mice on a diet high in saturated fat, fructose, and cholesterol. *Gastroenterology* 2016;151:733–746 e12.
5. Kiryluk K, Li Y, Scolari F, Sanna-Cherchi S, Choi M, Verbitsky M, Fasel D, Lata S, Prakash S, Shapiro S, Fischman C, Snyder HJ, Appel G, Izzi C, Viola BF, Dallera N, Del Vecchio L, Barlassina C, Salvi E, Bertinetto FE, Amoroso A, Savoldi S, Rocchietti M, Amore A, Peruzzi L, Coppo R, Salvadori M, Ravani P, Magistrini R, Ghiggeri GM, Caridi G, Bodria M, Lugani F, Allegri L, Delsante M, Maiorana M, Magnano A, Frasca G, Boer E, Boscutti G, Ponticelli C, Mignani R, Marcantoni C, Di Landro D, Santoro D, Pani A, Polci R, Feriozzi S, Chicca S, Galliani M, Gigante M, Gesualdo L, Zamboli P, Battaglia GG, Garozzo M, Maixnerova D, Tesar V, Eitner F, Rauen T, Floege J, Kovacs T, Nagy J, Mucha K, Paczek L, Zaniew M, Mizerska-Wasiak M, Roszkowska-Blaim M, Pawlaczyk K, Gale D, Barratt J, Thibaudin L, Berthoux F, Canaud G, Boland A, Metzger M, Panzer U, Suzuki H, Goto S, Narita I, Caliskan Y, Xie J, Hou P, Chen N, Zhang H, Wyatt RJ, Novak J, Julian BA, Feehally J, Stengel B, Cusi D, Lifton RP, Gharavi AG. Discovery of new risk loci for IgA nephropathy implicates genes involved in immunity against intestinal pathogens. *Nat Genet* 2014; 46:1187–1196.
6. Manfredo Vieira S, Hiltensperger M, Kumar V, Zegararuiz D, Dehner C, Khan N, Costa FRC, Tiniakou E, Greiling T, Ruff W, Barbieri A, Kriegel C, Mehta SS, Knight JR, Jain D, Goodman AL, Kriegel MA. Translocation of a gut pathobiont drives autoimmunity in mice and humans. *Science* 2018;359:1156–1161.
7. Potten CS. Keratinocyte stem cells, label-retaining cells and possible genome protection mechanisms. *J Invest Dermatol Symp Proc* 2004;9:183–195.
8. Withers HR. Regeneration of intestinal mucosa after irradiation. *Cancer* 1971;28:75–81.
9. Bismar MM, Sinicrope FA. Radiation enteritis. *Curr Gastroenterol Rep* 2002;4:361–365.
10. MacNaughton WK. Review article: new insights into the pathogenesis of radiation-induced intestinal dysfunction. *Aliment Pharmacol Ther* 2000;14:523–528.
11. Withers HR, Brennan JT, Elkind MM. The response of stem cells of intestinal mucosa to irradiation with 14 MeV neutrons. *Br J Radiol* 1970;43:796–801.
12. Cairnie AB, Millen BH. Fission of crypts in the small intestine of the irradiated mouse. *Cell Tissue Kinet* 1975; 8:189–196.
13. Sato T, Vries RG, Snippert HJ, van de Wetering M, Barker N, Stange DE, van Es JH, Abo A, Kujala P, Peters PJ, Clevers H. Single Lgr5 stem cells build crypt-villus structures in vitro without a mesenchymal niche. *Nature* 2009;459:262–265.
14. Bhanja P, Norris A, Gupta-Saraf P, Hoover A, Saha S. BCN057 induces intestinal stem cell repair and mitigates radiation-induced intestinal injury. *Stem Cell Res Ther* 2018;9:26.
15. Stokes K, Cooke A, Chang H, Weaver DR, Breault DT, Karpowicz P. The Circadian clock gene BMAL1 coordinates intestinal regeneration. *Cell Mol Gastroenterol Hepatol* 2017;4:95–114.
16. Yamauchi M, Otsuka K, Kondo H, Hamada N, Tomita M, Takahashi M, Nakasono S, Iwasaki T, Yoshida K. A novel in vitro survival assay of small intestinal stem cells after exposure to ionizing radiation. *J Radiat Res* 2014; 55:381–390.
17. Grabinger T, Luks L, Kostadinova F, Zimmerlin C, Medema JP, Leist M, Brunner T. Ex vivo culture of intestinal crypt organoids as a model system for assessing cell death induction in intestinal epithelial cells and enteropathy. *Cell Death Dis* 2014;5:e1228.
18. Sampson LL, Davis AK, Grogg MW, Zheng Y. mTOR disruption causes intestinal epithelial cell defects and

- intestinal atrophy postinjury in mice. *FASEB J* 2016; 30:1263–1275.
19. Merritt AJ, Potten CS, Kemp CJ, Hickman JA, Balmain A, Lane DP, Hall PA. The role of p53 in spontaneous and radiation-induced apoptosis in the gastrointestinal tract of normal and p53-deficient mice. *Cancer Res* 1994; 54:614–617.
 20. Gironella M, Malicet C, Cano C, Sandi MJ, Hamidi T, Taulil RM, Baston M, Valaco P, Moreno S, Lopez F, Neira JL, Dagorn JC, Iovanna JL. p8/nupr1 regulates DNA-repair activity after double-strand gamma irradiation-induced DNA damage. *J Cell Physiol* 2009; 221:594–602.
 21. Li X, Liu L, Yang S, Song N, Zhou X, Gao J, Yu N, Shan L, Wang Q, Liang J, Xuan C, Wang Y, Shang Y, Shi L. Histone demethylase KDM5B is a key regulator of genome stability. *Proc Natl Acad Sci U S A* 2014; 111:7096–7101.
 22. Qi W, Wang R, Chen H, Wang X, Xiao T, Boldogh I, Ba X, Han L, Zeng X. BRG1 promotes the repair of DNA double-strand breaks by facilitating the replacement of RPA with RAD51. *J Cell Sci* 2015;128:317–330.
 23. Maachani UB, Shankavaram U, Kramp T, Tofilon PJ, Camphausen K, Tandle AT. FOXM1 and STAT3 interaction confers radioresistance in glioblastoma cells. *Oncotarget* 2016;7:77365–77377.
 24. Ahn SH, Shah YM, Inoue J, Morimura K, Kim I, Yim S, Lambert G, Kurotani R, Nagashima K, Gonzalez FJ, Inoue Y. Hepatocyte nuclear factor 4alpha in the intestinal epithelial cells protects against inflammatory bowel disease. *Inflamm Bowel Dis* 2008;14:908–920.
 25. Pinto D, Gregorieff A, Begthel H, Clevers H. Canonical Wnt signals are essential for homeostasis of the intestinal epithelium. *Genes Dev* 2003;17:1709–1713.
 26. Babeu JP, Darsigny M, Lussier CR, Boudreau F. Hepatocyte nuclear factor 4alpha contributes to an intestinal epithelial phenotype in vitro and plays a partial role in mouse intestinal epithelium differentiation. *Am J Physiol Gastrointest Liver Physiol* 2009;297:G124–G134.
 27. Cattin AL, Le Beyec J, Barreau F, Saint-Just S, Houllier A, Gonzalez FJ, Robine S, Pincon-Raymond M, Cardot P, Lacasa M, Ribeiro A. Hepatocyte nuclear factor 4alpha, a key factor for homeostasis, cell architecture, and barrier function of the adult intestinal epithelium. *Mol Cell Biol* 2009;29:6294–6308.
 28. Mori-Akiyama Y, van den Born M, van Es JH, Hamilton SR, Adams HP, Zhang J, Clevers H, de Crombrughe B. SOX9 is required for the differentiation of Paneth cells in the intestinal epithelium. *Gastroenterology* 2007;133:539–546.
 29. Darsigny M, Babeu JP, Dupuis AA, Furth EE, Seidman EG, Levy E, Verdu EF, Gendron FP, Boudreau F. Loss of hepatocyte-nuclear-factor-4alpha affects colonic ion transport and causes chronic inflammation resembling inflammatory bowel disease in mice. *PLoS One* 2009;4:e7609.
 30. Ishihara H, Tanaka I, Yakumaru H, Tanaka M, Yokochi K, Akashi M. Pharmaceutical drugs supporting regeneration of small-intestinal mucosa severely damaged by ionizing radiation in mice. *J Radiat Res* 2013;54:1057–1064.
 31. Riehl TE, Alvarado D, Ee X, Zuckerman A, Foster L, Kapoor V, Thotala D, Ciorba MA, Stenson WF. Lactobacillus rhamnosus GG protects the intestinal epithelium from radiation injury through release of lipoteichoic acid, macrophage activation and the migration of mesenchymal stem cells. *Gut* 2019;68:1003–1013.
 32. UK IBD Genetics Consortium, Barrett JC, Lee JC, Lees CW, Prescott NJ, Anderson CA, Phillips A, Wesley E, Parnell K, Zhang H, Drummond H, Nimmo ER, Massey D, Blaszczyk K, Elliott T, Cotterill L, Dallal H, Lobo AJ, Mowat C, Sanderson JD, Jewell DP, Newman WG, Edwards C, Ahmad T, Mansfield JC, Satsangi J, Parkes M, Mathew CG, Wellcome Trust Case Control C, Donnelly P, Peltonen L, Blackwell JM, Bramer E, Brown MA, Casas JP, Corvin A, Craddock N, Deloukas P, Duncanson A, Jankowski J, Markus HS, Mathew CG, McCarthy MI, Palmer CN, Plomin R, Rautanen A, Sawcer SJ, Samani N, Trembath RC, Viswanathan AC, Wood N, Spencer CC, Barrett JC, Bellenguez C, Davison D, Freeman C, Strange A, Donnelly P, Langford C, Hunt SE, Edkins S, Gwilliam R, Blackburn H, Bumpstead SJ, Dronov S, Gillman M, Gray E, Hammond N, Jayakumar A, McCann OT, Liddle J, Perez ML, Potter SC, Ravindrarajah R, Ricketts M, Waller M, Weston P, Widaa S, Whittaker P, Deloukas P, Peltonen L, Mathew CG, Blackwell JM, Brown MA, Corvin A, McCarthy MI, Spencer CC, Attwood AP, Stephens J, Sambrook J, Ouwehand WH, McArdle WL, Ring SM, Strachan DP. Genome-wide association study of ulcerative colitis identifies three new susceptibility loci, including the HNF4A region. *Nat Genet* 2009;41:1330–1334.
 33. Farkas AE, Hilgarth RS, Capaldo CT, Gerner-Smidt C, Powell DR, Vertino PM, Koval M, Parkos CA, Nusrat A. HNF4alpha regulates claudin-7 protein expression during intestinal epithelial differentiation. *Am J Pathol* 2015; 185:2206–2218.
 34. Liu W, Li H, Hong SH, Piszczek GP, Chen W, Rodgers GP. Olfactomedin 4 deletion induces colon adenocarcinoma in Apc(Min/+) mice. *Oncogene* 2016; 35:5237–5247.
 35. Liu W, Yan M, Liu Y, Wang R, Li C, Deng C, Singh A, Coleman WG Jr, Rodgers GP. Olfactomedin 4 down-regulates innate immunity against Helicobacter pylori infection. *Proc Natl Acad Sci U S A* 2010; 107:11056–11061.
 36. Schmidt D, Wilson MD, Ballester B, Schwalie PC, Brown GD, Marshall A, Kutter C, Watt S, Martinez-Jimenez CP, Mackay S, Talianidis I, Flicek P, Odom DT. Five-vertebrate ChIP-seq reveals the evolutionary dynamics of transcription factor binding. *Science* 2010; 328:1036–1040.
 37. Kiselyuk A, Lee SH, Farber-Katz S, Zhang M, Athavankar S, Cohen T, Pinkerton AB, Ye M, Bushway P, Richardson AD, Hostetler HA, Rodriguez-Lee M, Huang L, Spangler B, Smith L, Higginbotham J, Cashman J, Freeze H, Itkin-Ansari P, Dawson MI, Schroeder F, Cang Y, Mercola M, Levine F. HNF4alpha antagonists discovered by a high-throughput screen for modulators of the human insulin promoter. *Chem Biol* 2012;19:806–818.

38. Tentu S, Nandarapu K, Muthuraj P, Venkitasamy K, Venkatraman G, Rayala SK. DHQZ-17, a potent inhibitor of the transcription factor HNF4A, suppresses tumorigenicity of head and neck squamous cell carcinoma in vivo. *J Cell Physiol* 2018;233:2613–2628.
39. Kim JH, Eom HJ, Lim G, Park S, Lee J, Nam S, Kim YH, Jeong JH. Differential effects, on oncogenic pathway signalling, by derivatives of the HNF4 alpha inhibitor BI6015. *Br J Cancer* 2019;120:488–498.
40. Hayhurst GP, Lee YH, Lambert G, Ward JM, Gonzalez FJ. Hepatocyte nuclear factor 4alpha (nuclear receptor 2A1) is essential for maintenance of hepatic gene expression and lipid homeostasis. *Mol Cell Biol* 2001;21:1393–1403.

Received September 13, 2019. Accepted February 25, 2020.

Correspondence

Address correspondence to: Vanesa Muncan, PhD, Tytgat Institute for Liver and Intestinal Research, Department of Gastroenterology and Hepatology,

Amsterdam Gastroenterology and Metabolism, Amsterdam UMC, University of Amsterdam, Meibergdreef 69-71, Amsterdam, The Netherlands. e-mail: v.muncan@amsterdamumc.nl; fax: (31) 20-566-9190.

Author contributions

Paula S. Montenegro-Miranda, Jonathan H. M. van der Meer, Gijs R. van den Brink, and Vanesa Muncan designed the study; Paula S. Montenegro-Miranda, Jonathan H. M. van der Meer, Christine Jones, Sander Meisner, Jacqueline L. M. Vermeulen, Jan Koster, and Vanesa Muncan collected and/or analyzed the data; Paula S. Montenegro-Miranda, Jonathan H. M. van der Meer, Christine Jones, Manon E. Wildenberg, Jarom Heijmans, Francois Boudreau, Agnes Ribeiro, Gijs R. van den Brink, and Vanesa Muncan interpreted the data; Paula S. Montenegro-Miranda, Jonathan H. M. van der Meer, Gijs R. van den Brink, and Vanesa Muncan drafted the manuscript; and Christine Jones, Sander Meisner, Jacqueline L. M. Vermeulen, Jan Koster, Manon E. Wildenberg, Jarom Heijmans, Agnes Ribeiro, and Francois Boudreau co-authored the writing of the manuscript. All authors edited the manuscript and read and approved the final manuscript.

Conflicts of interest

Gijs R. van den Brink is an employee of Roche. All other authors have nothing to disclose.

Funding

This work was financially supported by Vici grant 016.140.605 from the Netherlands Organisation for Scientific Research (G.R.v.d.B.).